ResearchGate

See discussions, stats, and author profiles for this publication at: https://www.researchgate.net/publication/11361350

Structural organization of the fibrin(ogen) alpha C-domain.

ARTICLE *in* BIOCHEMISTRY · JUNE 2002

Impact Factor: 3.02 · Source: PubMed

CITATIONS
29

READS
22

3 AUTHORS, INCLUDING:

Leonid Medved
University of Maryland, Baltimore
118 PUBLICATIONS **3,010** CITATIONS

SEE PROFILE

Available from: Leonid Medved
Retrieved on: 25 January 2016

Structural Organization of the Fibrin(ogen) αC-Domain†

Galina Tsurupa,‡ Latchezar Tsonev,§ and Leonid Medved*,‡

Department of Biochemistry, The American Red Cross Holland Laboratory, Rockville, Maryland 20855, and Resuscitative Medicine Department, Transfusion and Cryopreservation Research Program, Naval Medical Research Center, Silver Spring, Maryland 20910

Received January 24, 2002; Revised Manuscript Received March 20, 2002

ABSTRACT: We hypothesized that the αC-domain of human fibrinogen (residues hAα221−610) and of other species consists of a compact COOH-terminal region (hAα392−610) and a flexible NH_2-terminal connector region (hAα221−391) which may contain some regular structure [Weisel and Medved (2001) *Ann. N.Y. Acad. Sci. 936*, 312−327]. To test this hypothesis, we expressed in *E. coli* recombinant fragments corresponding to the full-length human αC-domain and its NH_2- and COOH-terminal regions as well as their bovine counterparts, bAα224−568, bAα224−373, and bAα374−568(538), respectively, and tested their folding status by fluorescence spectroscopy, circular dichroism (CD), and differential scanning calorimetry (DSC). All three methods revealed heat-induced unfolding transitions in the full-length bAα224−568 and its two COOH-terminal fragments, indicating that the COOH-terminal portion of the bovine αC-domain is folded into a compact cooperative structure. Similar results were obtained by CD and DSC with the full-length and the COOH-terminal h392−610 human fragments. The NH_2-terminal fragments of both species, b224−373 and h221−392, did not exhibit any sign of a compact structure. However, their heat capacity functions, CD spectra, and temperature dependence of ellipticity at 222 nm were typical for peptides in the extended helical poly(L-proline) type II conformation (PPII), suggesting that they contain this type of regular structure. This is consistent with the presence of proline-rich tandem repeats in the sequence of both bovine and human connector regions. These results indicate that both bovine and human fibrinogen αC-domains consist of a compact globular cooperative unit attached to the bulk of the molecule by an extended NH_2-terminal connector region with a PPII conformation.

Fibrinogen is a plasma protein that after thrombin-mediated activation forms fibrin clots, preventing the loss of blood upon vascular injury or causing thrombosis in pathological states. In addition to its prominent role in hemostasis, fibrin(ogen) plays an important role in cell adhesion, migration, and proliferation during wound healing, inflammation, angiogenesis, and tumorigenesis. Such a multifunctional character of fibrin(ogen) is connected with its complex structure that accommodates multiple binding sites providing its participation in the above-mentioned processes. A comprehensive understanding of its biological functions requires detailed knowledge of its structural organization.

The chemical structure of fibrinogen was established in numerous biochemical studies. According to the current view, fibrinogen consists of two identical subunits, each of which is formed by three nonidentical polypeptide chains, Aα, Bβ, and γ (*1*, *2*). Both the subunits and the chains are linked together by disulfide bonds, and assemble to form at least 20 distinct domains (*3*−*5*) grouped into 4 major structural regions: the central E region, 2 identical terminal D regions, and the αC-domains. The central E region is a chemical dimer formed by the NH_2-terminal portions of all six chains, while the distal D regions are formed by the COOH-terminal portions of the Bβ and γ chains and a portion of the Aα chains. The D-E-D arrangement corresponds to the three major nodules revealed by electron microscopy of intact fibrinogen (*6*); a fourth nodule observed in some molecules (*7*, *8*) was suggested to correspond to two interacting αC-domains, each made up of the COOH-terminal two-thirds of the Aα chain.

Plasmin and some other proteases cleave fibrinogen to produce two fragments D and one fragment E corresponding to the D and E regions, respectively, while the αC-domains are cleaved into a smaller fragments (*1*, *2*). The D and E fragments, which account for two-thirds of the molecule, preserve compact structure and proved to be extremely useful in elucidation of fibrin(ogen) structure and functions. Significant progress has been made recently in determining the three-dimensional structure of fibrinogen. First, high-resolution structures of human fibrinogen fragment D and its cross-linked dimer from fibrin were established (*9*, *10*) followed by a high-resolution structure of bovine fibrinogen E fragment including most of the central region E (*11*). Second, an overall picture of the fibrinogen molecule at low 4.0 Å resolution was obtained from a crystallographic study of proteolytically modified bovine fibrinogen (*12*). Further, the structure of native chicken fibrinogen was solved at 5.5 Å

† This work was supported by National Institutes of Health Grant HL-56051 (to L.M.).

* To whom correspondence should be addressed at The Holland Laboratory, American Red Cross, 15601 Crabbs Branch Way, Rockville, MD 20855. Tel: 301-738-0719. Fax: 301-738-0740. E-mail: medvedL@usa.redcross.org.

‡ The American Red Cross Holland Laboratory.

§ Naval Medical Research Center.

10.1021/bi025584r CCC: $22.00 © 2002 American Chemical Society
Published on Web 04/27/2002

and then at higher 2.7 Å resolution (*13, 14*). In these studies, the D regions and most of the E region were well-resolved, making available a high-resolution structure of about two-thirds of the 340 kDa fibrinogen molecule. The structure of two 40 kDa αC-domains comprising about one-fourth of the mass of the molecule remains to be established.

Having established the crystal structure of the D and E fragments, it would be reasonable to attempt crystallization of the αC-domain for X-ray analysis. However, the question whether this domain even contains compact structure is still debated. On one hand, early calorimetric studies of bovine fibrinogen and its fragment X lacking the COOH-terminal region of the Aα chains revealed an extra heat absorption peak in the endotherm of the former which was assigned to melting of the two interacting αC-domains (*3*). These domains are thought to account for the extra nodule in electron micrographs of bovine and human fibrinogens (*5, 7, 8, 15*). Sequence analysis of the human αC-domain (residues Aα221−610) also predicted a high probability of compact structure in its COOH-terminal half and a low probability in the NH_2-terminal half (*5*). These studies resulted in the hypothesis that each αC-domain consists of a compact COOH-terminal half attached to the bulk of the molecule via an unordered NH_2-terminal half (connector region). However, the additional heat absorption peak was not observed in the endotherm of human fibrinogen (*16*), and there was no convincing evidence for the presence of a compact structure in the recombinant human fibrinogen αC-domain (*17*). Moreover, in a recent X-ray study of native chicken fibrinogen, the αC-domains were not visible in electron density maps, leading to the conclusion that their structure is very disordered (*13, 14*).

To interpret the above-mentioned conflicting observations, one should take into account that they were obtained with fibrinogens from different species in which the length and the sequence of the αC-domains vary substantially and thus may have different structural organizations. In addition, none of those observations can be regarded as final evidence for the presence or absence of compact structure in the αC-domain. To address this question, it is necessary to test the folding status of the isolated αC-domains of different species in direct experiments. In this study, we expressed both bovine and human fibrinogen αC-domains as well as their truncated variants and investigated their folding properties by various methods. The results provide direct evidence for the presence of compact cooperative structure in the αC-domain of both species and suggest that the connector region may contain some ordered noncooperative structure. They also identify a minimal region in the αC-domain that is folded into a compact structure and could be a good candidate for crystallization.

EXPERIMENTAL PROCEDURES

Human Fibrinogen Fragments and Peptide. The recombinant human fibrinogen αC-fragments, h221−610, h221−391, and h392−610, corresponding to the full-length human αC-domain and its NH_2- and COOH-terminal portions, respectively, were produced in *E. coli* using the pET-20b expression vector as described earlier (*17, 18*).

A synthetic peptide, NPGSPRPGSTGT, corresponding to residues 329−340 of the human fibrinogen Aα chain (sixth repeat in the connector region of the αC-domain) was synthesized by SynPep (Dublin, CA).

Expression and Purification of Recombinant Bovine Fibrinogen αC-Fragments. Recombinant bovine fibrinogen αC-fragments, b224−568, b224−373, b374−538, and b374−568, corresponding to the full-length bovine αC-domain and its NH_2-terminal portion and COOH-terminal truncated variants, respectively, were expressed in *E. coli* using the pET-20b expression vector (Novagen Inc.). A fragment of cDNA encoding bovine fibrinogen Aα chain kindly provided by Dr. Murakawa was used as a template to amplify by polymerase chain reaction a cDNA encoding bovine αC-fragments. The following oligonucleotides were used as primers: 5′-AGAGACATATGCAGCTCCAAGAGGCCCC-3′ and 5′-AGAGAAAGCTTCTAGGCAGGACGAGCTT-TAGTATG-3′ for the b224−568 fragment; 5′-AGAGA-CATATGCAGCTCCAAGAGGCCCC-3′ and 5′-AGA-GAAAGCTTCTACCAGTCTGGACTGGAAGG-3′ for the b224−373 fragment; 5′-AGAGACATATGGGCACCTTTA-GAGAGGAAG-3′ and 5′-AGAGAAAGCTTCTAAAAGT-GCTTGCTTTCAATCGC-3′ for the b374−538 fragment; 5′-AGAGACATATGGGCACCTTTAGAGAGGAAG-3′ and 5′-AGAGAAAGCTTCTAGGCAGGACGAGCTTTAGTA-TG-3′ for the b374−568 fragment. The forward primers incorporated the *Nde*I restriction site immediately before the coding region; the final three bases of the *Nde*I site, ATG, code for the fMet residue that initiates translation (*19*). The reverse primers included a TAA stop codon immediately after the coding segment, following by a *Hin*dIII site. The amplified cDNA fragments were purified by electrophoresis in an agarose gel, digested with *Nde*I and *Hin*dIII restriction enzymes, and ligated into the pET-20b expression vector. The resulting plasmids were used for transformation of DH5α and then B834(DE3) pLysS *E. coli* host cells. All cDNA fragments were sequenced in both directions to confirm the integrity of the coding sequences.

All bovine αC-fragments were found in inclusion bodies from which they were purified by the procedure described earlier for the human αC-fragments (*18*). Taking into account that the αC-domain is highly susceptible to proteolysis, all bovine and human fragments were analyzed by SDS−PAGE and sequenced for six cycles after purification to confirm their integrity. NH_2-terminal sequence analysis was performed with a Hewlett-Packard model G1000A protein sequencer.

Refolding of the Recombinant Fragments. When tested by SDS−PAGE, the recombinant bovine fragments containing two Cys residues had slightly decreased mobility upon reduction (not shown), indicating that their Cys^{423}−Cys^{473} disulfide bond was intact, as with the recombinant human αC-fragments described earlier (*17*). Therefore, the purified fragments were refolded by slow dialysis from urea without any reducing agent. In the case of the full-length b224−568 and h221−610 fragments, and their connector fragments, b224−373 and h221−391, the proteins in 6 M urea were diluted 10-fold with 8 M urea to a final concentration of 10 μM and dialyzed against a 4-fold volume of 8 M urea at 4 °C for several hours. Then the concentration of urea in the container was slowly reduced to 0.8 M by addition of 20 mM Tris buffer, pH 8.0, containing 2 M NaCl, over a period of 18 h at 4 °C. The subsequent 10-fold reduction of urea concentration was performed in the same manner using 20

mM Tris buffer, pH 8.0, with 0.15 M NaCl, followed by extensive dialysis of the proteins versus the same buffer. In the case of COOH-terminal variants, the b374−538, b374−568, and h392−610 fragments, slow dialysis was done in one step. The concentration of urea in the container was slowly reduced from 8 to 0.08 M by addition of 20 mM Tris buffer, pH 8.0, containing 2 M NaCl, over a period of 36 h at 4 °C followed by extensive dialysis of the fragments versus the same buffer. Residual insoluble material observed in some samples was removed by centrifugation. All refolded fragments were concentrated to 1.0−3.0 mg/mL with a Centriprep 10 concentrator (Millipore), filtered through 0.2 μm filter unit, and stored at 4 °C.

Protein Concentration Determination. Concentrations of the recombinant fragments were determined spectrophotometrically using extinction coefficients ($E_{280,1\%}$) calculated from the amino acid composition with the equation: $E_{280,1\%} = (5690W + 1280Y + 120S{-}S)/(0.1\ M)$, where W, Y, and $S{-}S$ represent the number of Trp and Tyr residues and disulfide bonds, respectively, and M represents the molecular mass (*20, 21*). Molecular masses of the recombinant fragments were calculated based on their amino acid composition. The following values of molecular masses and $E_{280,1\%}$ were obtained: 36.6 kDa and 12.8 for the b224−568 fragment; 15.4 kDa and 26.6 for the b224−373 fragment; 18.1 kDa and 3.2 for the b374−538 fragment; 21.3 kDa and 2.7 for the b374−568 fragment; 40.9 kDa and 12.7 for the h221−610 fragment; 17.4 kDa and 26.9 for the h221−391 fragment, and 23.6 kDa and 2.2 for the h392−610 fragment. Note that these values take into account the NH_2-terminal fMet residue present in all recombinant fragments (see above) while the numbering of the fragments does not.

Fluorescence Study. Fluorescence spectra were recorded in an SLM 8000-C fluorometer. Fluorescence measurements of thermal- or chemical-induced unfolding were performed by monitoring the ratio of the intensity at 370 nm to that at 330 nm with excitation at 280 nm in the same fluorometer. Temperature was controlled with a circulating water bath programmed to raise the temperature at 1 °C/min. Protein concentrations were 0.02−0.1 mg/mL. Urea-induced unfolding was accomplished in the same instrument at room temperature by continuous addition with a motorized syringe of a concentrated stock solution of the titrant (8 M urea) at a rate of 20 μL/min to a stirred cuvette containing the protein solution at 0.02−0.1 mg/mL while monitoring the fluorescence ratio as described above. Both the fluorometer and the syringe-driver were controlled by a computer, which automatically corrected the fluorescence intensity for dilution assuming a linear dependence on protein concentration below 0.15 mg/mL.

Circular Dichroism Measurements. Circular dichroism (CD)[1] spectra were continuously recorded on a Jasco-715 spectropolarimeter while the temperature was simultaneously ramped between 0 and 100 °C at a rate of 1 °C/min using a computer-controlled circulating water bath (Julabo, Germany). All experiments were carried out in quartz cuvettes of 0.02 or 0.5 cm path length for the far-UV or the near-UV range, respectively, and protein concentrations between 1 and 2.5 mg/mL. Proteins were dissolved in 20 mM Tris buffer, pH 7.4, with 0.15 M NaCl, or in 10 mM phosphate buffer, pH 7.4.

Determination of Apparent van't Hoff Enthalpy. Values of the apparent van't Hoff enthalpy (ΔH_{vH}) were estimated from the heat-induced melting curves registered by fluorescence or CD as follows. Data in the pre- and post-transition regions of the denaturation curves were fit to straight lines by linear regression. The resulting parameters were used to predict the values of the fluorescence ratio or ellipticity for the native and denatured states in the transition region. The apparent fraction denatured, f, at any point in the transition region was then calculated by interpolation. This allowed the calculation of an apparent equilibrium constant, $K = f/(1 - f)$, whose logarithm was then plotted against the inverse temperature (K). The resulting van't Hoff plots were fitted by linear regression, and the apparent ΔH_{vH} was calculated from the slope. Such analysis is based on the assumption that the change in fluorescence ratio or ellipticity is directly proportional to the fraction of the entire protein that has been converted from the fully native to the fully denatured state.

Calorimetric Study. Differential scanning calorimetry (DSC) measurements were made with DASM-4M calorimeter (*22*) in the temperature range 10−100 °C at a scan rate of 1 °C/min and protein concentrations of 2.5−3.5 mg/mL. The DSC curves were corrected for an instrumental baseline obtained by heating the buffer. Melting temperatures (T_m) and the calorimetric and van't Hoff enthalpies of denaturation were determined from the DSC curves using software provided by Dr. V. Filimonov (Institute of Protein Research, Pushchino, Russia). Deconvolution analysis was performed according to (*22, 23*) using the same software. The values of the theoretical heat capacities of the unfolded fragments were calculated as in (*24, 25*).

RESULTS

Preparation and Refolding of the αC-Fragments. The human fibrinogen αC-domain (Aα221−610) consists of the NH_2-terminal connector region including residues 221−391 followed by the COOH-terminal half (residues 392−610) which was proposed to be compact (*5*). The bovine fibrinogen αC-domain (Aα224−568) is smaller due to deletion of several regions as revealed by alignment of the human and bovine sequences (Figure 1A). In this study the full-length human and bovine αC-domains, h221−610 and b224−568, respectively, and their homologous NH_2- and COOH-terminal halves, h221−391, b224−373 and h392−610, b374−568, respectively (Figure 1B), were expressed in bacteria, and their folding properties were tested by various methods. In addition, the b374−538 fragment lacking the 3 kDa COOH-terminal region was also expressed and analyzed.

Since all fragments except the human connector (h221−391) were found in inclusion bodies, their solubilization in urea and subsequent refolding was a critical step in preparation of the folded proteins. We first developed a refolding procedure for the full-length bovine αC-fragment and its COOH-terminal variants since, in contrast to the human ones, they contain a single Trp residue in their COOH-terminal part, which allowed the refolding to be monitored by fluorescence. Among various refolding conditions tested, those described under Experimental Procedures yielded

[1] Abbreviations: CD, circular dichroism; DSC, differential scanning calorimetry; PPII, extended left-handed helical poly(L-proline) type II conformation; ΔH_{vH}, apparent van't Hoff enthalpy.

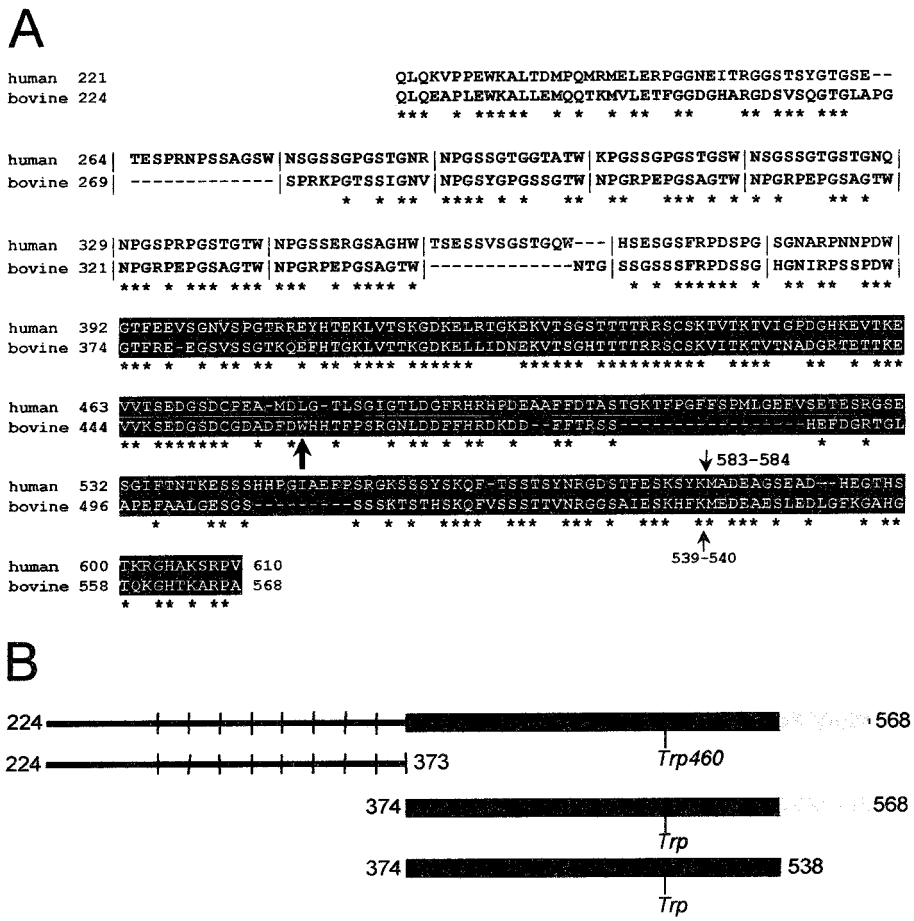

FIGURE 1: Alignment of the human and bovine fibrinogen αC-domain sequences and schematic representation of the recombinant bovine αC-domain variants. Panel A: alignment of the sequences performed with the Vector NTI 6.0 program. Aligned identical residues are depicted by stars; deletions are represented by dashed lines. The vertical bars in the NH_2-terminal connector regions denote the 13-residue tandem repeats. The COOH-terminal regions are presented on a black background, and Trp460, the only Trp residue in this region of bovine αC-fragment, is indicated by the thick arrow. The thin arrows indicate plasmin cleavage sites in the extreme COOH-terminal region of human and bovine αC-domains at residues 583−584 and 539−540, respectively. Panel B: schematic representation of the recombinant bovine full-length αC-domain and its truncated variants expressed for this study. The COOH-terminal region is highlighted by the black-and-gray box; the boundaries between the tandem repeats in the NH_2-terminal connector region are presented by the vertical bars.

fragments whose fluorescence spectra in the final "native" buffer had maxima at 347−348 nm (vs 350−352 nm in 8 M urea), suggesting the presence of a folded structure. Only the fragments with such spectra were used for further structural studies. The refolding procedure developed for the bovine αC-fragments was then applied for refolding of the human counterparts.

Fluorescence-Detected Denaturation of the Bovine αC-Fragment and Its Variants. To test the refolded bovine αC-fragments for compact structure, we performed a fluorescence study of their heat-induced unfolding. Figure 2A presents melting curves obtained by heating the fragments in glycine buffer while monitoring the ratio of fluorescence intensity at 370 nm to that at 330 nm as a measure of the spectral shift that accompanies unfolding. Under such conditions, the full-length b224−568 fragment and its COOH-terminal variants, b374−568 and b374−538, exhibited sigmoidal denaturation transitions while no such transition was observed in the NH_2-terminal variant, b224−373, corresponding to the connector region. These results indicate that the full-length bovine αC-fragment and its COOH-terminal fragments contain compact cooperative structure[2] while the connector fragment does not. The urea-induced denaturation experiments whose results are presented in Figure 2B confirmed this finding.

Visual inspection of the thermally induced transitions shows that the b224−568 and b374−538 fragments have similar stability and that the sharpness of these transitions, which reflects the cooperativity of the melting process, is also similar. The transition in the b374−568 fragment seems to occur in the same temperature range, although its amplitude was almost 2-fold lower. The similarity becomes more evident when the data are transformed to yield the fraction denatured as shown in the inset in Figure 2A. The midpoints (T_m) of the transitions for all three fragments were found to be very close, at 40−43 °C. The "apparent" van't Hoff enthalpies (ΔH_{vH}) calculated from the fraction denatured (see Experimental Procedures) were also similar, in the range of 33−40 kcal/mol. Such similarity suggests that the same structure unfolds in all three fragments, i.e., that this structure is formed by the COOH-terminal region of the αC-domain.

[2] By cooperative structure, we mean a structure that is compact and independently folded as evidenced by the fact that it unfolds in a cooperative all-or-none manner, giving rise to a sigmoidal transition (*56*).

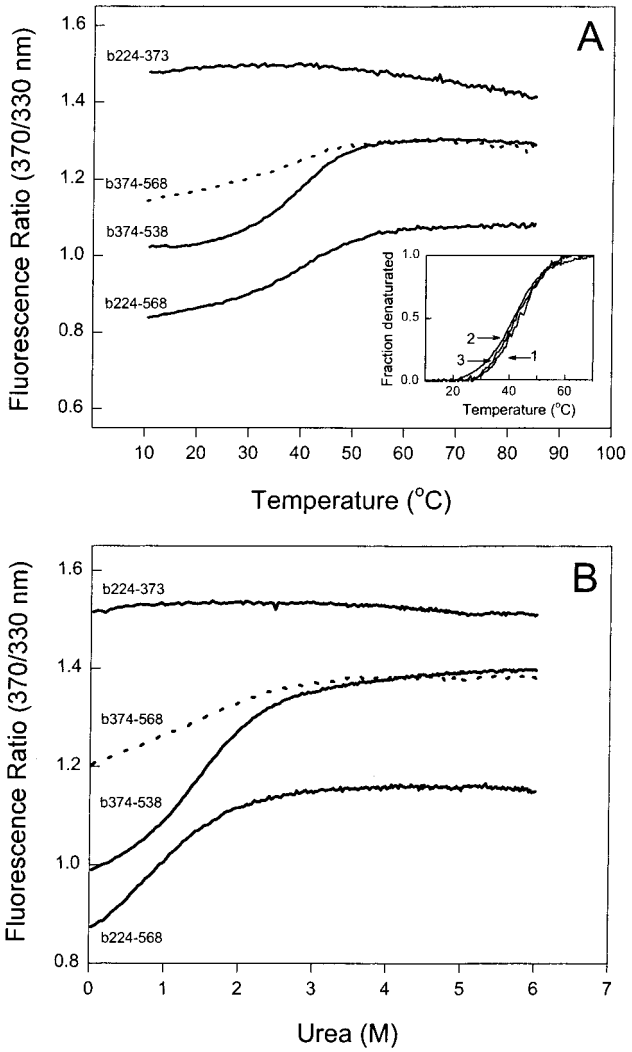

FIGURE 2: Fluorescence-detected denaturation of the recombinant bovine αC-fragment and its truncated variants. Panel A: melting curves obtained upon heating of the b224−568, b224−373, b374−538, and b374−568 fragments in 20 mM Gly buffer, pH 8.5, containing 150 mM NaCl. The curves for b224−568 (1), b374−538 (2), and b374−568 (3) which have been transformed to give the fraction denatured as a function of temperature (see Experimental Procedures) are presented in the inset. Panel B: urea-induced denaturation curves of the same αC-fragments in the same buffer as in panel A. All curves were arbitrarily shifted along the vertical axis to improve visibility.

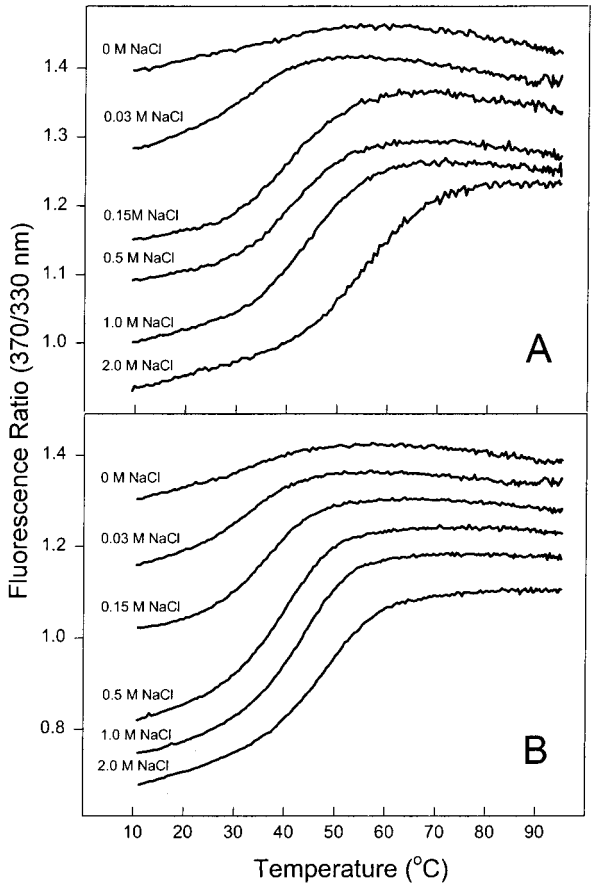

FIGURE 3: Fluorescence-detected thermal denaturation of the recombinant bovine αC-fragment and its COOH-terminal truncated variant at various concentrations of sodium chloride. Panels A and B show melting curves obtained upon heating of the b224−568 and b374−538 fragments, respectively. All experiments were performed in 20 mM Gly buffer, pH 8.5, containing the indicated concentrations of NaCl. All curves were arbitrarily shifted along the vertical axis to improve visibility.

Since the presence of NaCl was required for successful refolding of the bovine αC-fragments (see Experimental Procedures), we studied thermal denaturation of the full-length αC-fragment (b224−568) and its compact truncated variant (b374−538) at different salt concentrations to evaluate the influence on their stabilities. The results presented in Figure 3 revealed that the stability of both fragments increased with increasing concentration of NaCl up to 2 M. At subphysiological salt concentration, the stability as well as the amplitude of the transition was decreased. These results show that NaCl stabilizes compact structure in both fragments.

CD-Detected Thermal Denaturation of the Bovine αC-Fragments. To further characterize the structure of the bovine αC-fragments, we studied their heat-induced unfolding by circular dichroism (CD). Based on the above finding of the stabilizing effect of salt, the CD measurements were carried out in buffer containing 0.15 M NaCl, although the latter interfered with the CD signal, precluding the acquisition of data below 200 nm. While CD spectra in the far-UV region are connected with the presence of secondary structure, those in the near-UV region, which usually have much lower amplitude, are connected with tertiary structure, reflecting an asymmetry in the environment of aromatic residues. In the near-UV region, all αC-fragments at low temperature exhibited CD spectra with positive maxima at 276−278 nm whose amplitudes were decreased at high temperature (see insets in Figure 4). This decrease occurred in a sigmoidal manner in the b224−568, b374−568, and b374−538 fragments, indicating cooperative unfolding of some tertiary structure, while in the case of the connector (b224−373) the change of the CD signal was linear (Figure 4C), suggesting the absence of such structure.

In the far-UV region at low temperature, the full-length αC-fragment and its COOH-terminal variants exhibited CD spectra with a negative shoulder at 210−240 nm whose amplitude increased with increasing temperature (insets in Figure 5A,B). When fragments were heated while monitoring ellipticity at 222 nm, a weak sigmoidal transition was observed with the full-length αC-domain (Figure 5A). A similar transition but more pronounced was observed in the case of the COOH-terminal b374−538 and b374−568

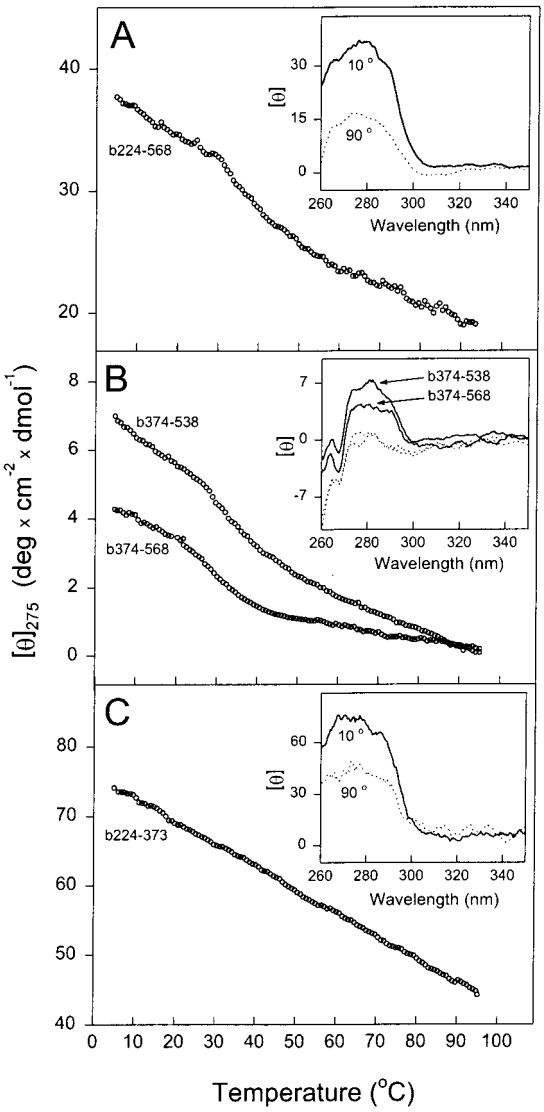

FIGURE 4: Thermal denaturation of the recombinant bovine αC-fragment and its truncated variants detected by circular dichroism in the near-UV region. Panel A shows changes in ellipticity at 275 nm upon heating of the b224−568 fragment in 20 mM Tris buffer, pH 8.0, with 150 mM NaCl. Panel B shows the same for the b374−568 and b374−538 fragments in the same buffer. Panel C refers to the b224−373 fragment in 20 mM sodium phosphate buffer, pH 7.4. The CD spectra in the near-UV region of the fragments at 10 °C (solid lines) and 90 °C (dotted lines) are presented in the corresponding insets.

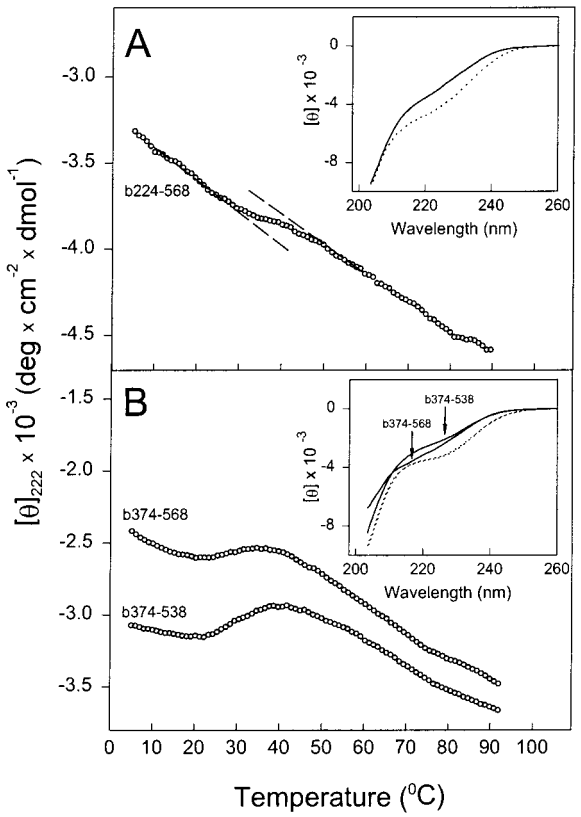

FIGURE 5: Thermal denaturation of the recombinant bovine αC-fragment and its truncated COOH-terminal variants detected by circular dichroism in the far-UV region. Panel A: heat-induced changes in ellipticity at 222 nm of the b224−568 fragment. The dashed lines represent linear extrapolations of the CD values before and after transition to highlight its sigmoidal character. Panel B: changes in ellipticity at 222 nm of the b374−568 and b374−538 fragments. The CD spectra in the far-UV region of all these fragments at 10 °C (solid lines) and 90 °C (dotted lines) are presented in the corresponding insets; those for the b374−568 and b374−538 essentially coincide at 90 °C. All experiments were performed in 20 mM Tris buffer, pH 8.0, with 150 mM NaCl.

fragments which do not contain the connector region (Figure 5B). These results clearly indicate unfolding of the secondary structure that contributes at this wavelength.

In the near-UV region, the sigmoidal transitions for all three fragments that contain the COOH-terminal portion (b224−568, b374−538, and b374−568) occurred in the same temperature range with T_ms at 39−40 °C, close to those observed by fluorescence. The values of the apparent van't Hoff enthalpies calculated for each fragment (see Experimental Procedures) were found to be in the range of 32−40 kcal/mol, close to those determined from the fluorescence-detected transitions. In the far-UV region, the transitions in all three fragments also occurred in the same temperature range although the values of the T_ms were lower, 34−36 °C. The similarity in T_ms and the apparent van't Hoff enthalpies of denaturation for the studied fragments indicate that the COOH-terminal region of the αC-domain contains secondary and tertiary structure which unfolds in a cooperative manner, reinforcing the previous conclusion about the presence of compact structure in this region based on fluorescence measurements. In addition, together with the fluorescence data they suggest that the Aα539−568 region missing in the b374−538 fragment does not contribute noticeably to the stability of the compact structure in the bovine αC-domain and that the Aα374−538 region of the latter is sufficient to form such structure.

DSC-Detected Thermal Denaturation of the Bovine αC-Fragments. Differential scanning calorimetry allows measurement of integral heat absorbed upon denaturation and provides more information about the unfolding process. However, because DSC requires higher concentration of proteins, we were able to apply this technique only to the COOH-terminal truncated b374−538 fragment and the b224−373 connector; the solubility of the full-length bovine αC-fragment and the b374−568 fragment was not sufficient to reach the concentration required for the calorimeter. When heated in the calorimeter, the b374−538 fragment exhibited a prominent heat absorption peak whose stability and amplitude increased at higher salt concentration (Figure 6A, middle and upper curves), in agreement with the fluorescence

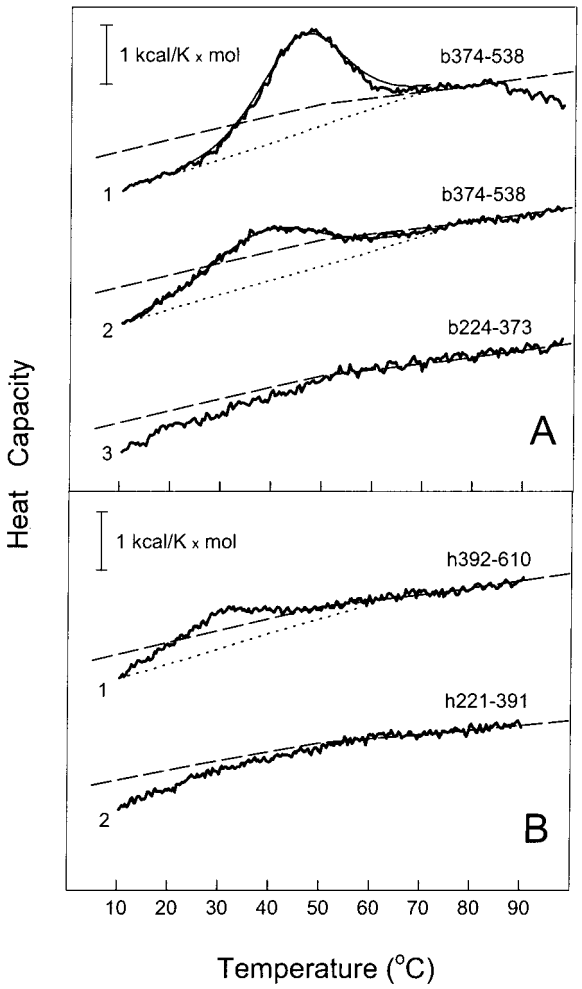

FIGURE 6: Thermal denaturation of the recombinant bovine and human αC-fragment variants detected by differential scanning calorimetry. Panel A: the solid uneven lines represent original DSC curves of the recombinant bovine b374−538 fragment in 20 mM Gly, pH 8.5, in the presence of 2 M NaCl (curve 1) or 0.15 M NaCl (curve 2), and the b224−373 fragment in 20 mM Gly buffer, pH 8.5 (curve 3). The dotted lines indicate the manner in which the excess heat capacity function for each curve was determined to derive calorimetric enthalpy; the thin solid lines, which essentially coincide with the experimental uneven lines, represent the best fits by a two-state transition. Panel B: the solid uneven lines represent original DSC curves of the recombinant human h392−610 fragment in 20 mM Gly buffer, pH 8.5, with 0.5 M NaCl (curve 1), and the h221−391 fragment in 20 mM Gly buffer, pH 8.5 (curve 2). The dashed lines in both panels represent the theoretical heat capacity functions for the unfolded fragments calculated as described under Experimental Procedures.

data. In contrast, the connector fragment exhibited no such peak (Figure 6A, lower curve). The transitions detected at low and high salt concentrations occurred at 39.6 and 46.1 °C, respectively, and the calorimetric enthalpies of denaturation determined directly in the experiments were found to be respectively 24 and 32 kcal/mol. The van't Hoff enthalpies determined from the shape of the curves were found to be 28 and 40 kcal/mol, close to the respective calorimetric enthalpies and also to the apparent van't Hoff enthalpies determined from the fluorescence- and CD-obtained melting curves (see above). This suggests that we are dealing with the unfolding of one cooperative unit. In agreement, the endotherms obtained at low and high salt concentrations were fitted well by one two-state transition with enthalpies of 25 and 35 kcal/mol, respectively. Thus, the thermodynamic

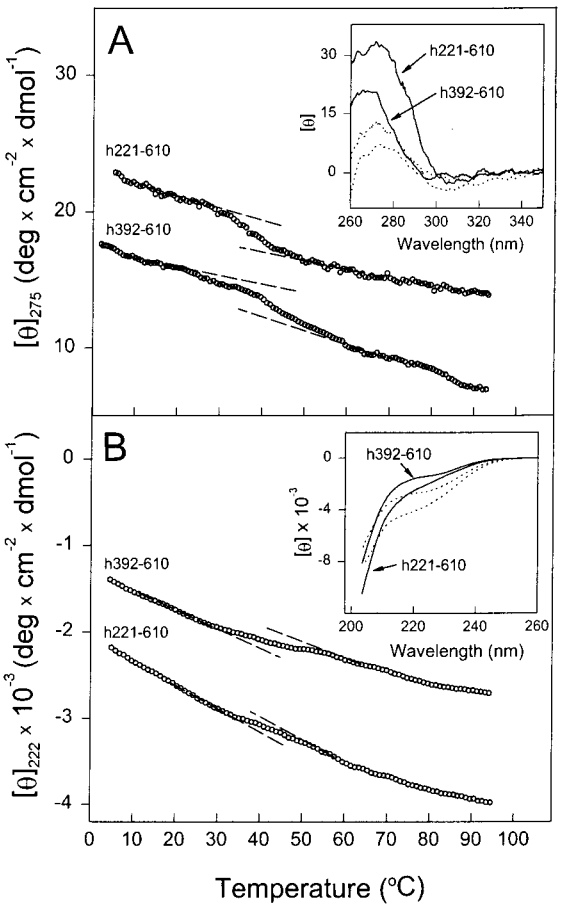

FIGURE 7: Thermal denaturation of the recombinant human αC-fragment and its truncated COOH-terminal variant detected by circular dichroism. Panel A: heat-induced changes in ellipticity at 275 nm of the h221−610 and h392−610 fragments. Panel B: changes in ellipticity of the same fragments at 222 nm. The near- and far-UV CD spectra of these fragments at 10 °C (solid lines) and 90 °C (dotted lines) are shown in the corresponding insets. The dashed lines represent linear extrapolations of the CD values before and after transitions to highlight their sigmoidal character. All experiments were performed in 20 mM Tris buffer, pH 8.0, with 150 mM NaCl.

analysis of the DSC-detected endotherms indicates unfolding in the full-length bovine αC-domain of a single cooperative unit which is formed by its COOH-terminal part.

Thermal Denaturation of the Human αC-Fragments. Since the COOH-terminal half of the human αC-fragment does not contain Trp, we utilized only CD and DSC to test its folding status. Similarly to the bovine αC-fragments, the human h221−610 and h392−610 fragments both exhibited sigmoidal thermal transitions in the far- and near-UV regions upon heating, indicating cooperative unfolding of the secondary and tertiary structures (Figure 7 A,B). In both near- and far-UV regions, the transitions for the full-length αC-fragment and its COOH-terminal variant occurred in the same temperature range (T_m = 42−43 °C). The values of the apparent van't Hoff enthalpy for both fragments calculated from the fraction denatured were also similar. These values (ΔH_{vH} = 36−37 kcal/mol) were comparable with those obtained for the corresponding bovine αC-fragments.

As in the case with the full-length bovine αC-fragment, it was impossible to reach a concentration of the full-length human αC-fragment sufficient for DSC measurements while the COOH-terminal h392−610 fragment and human con-

nector were adequately soluble. When heated in the calorimeter, the h392−610 fragment exhibited a weak heat absorption peak, suggesting unfolding of a compact structure (upper curve in Figure 6B). However, the T_m of this peak (32 °C) and the experimentally determined calorimetric enthalpy (16 kcal/mol) were substantially lower than those determined for this fragment in the CD experiments, although the van't Hoff enthalpy determined from the shape of the transition (ΔH_{vH} = 31 kcal/mol) was comparable. Because of these discrepancies, no attempt was made to further analyze this endotherm. A possible explanation for the low heat effect and the discrepancy between calorimetric and van't Hoff enthalpies could be that part of the protein was not properly folded because the refolding procedure developed here for bovine fragments may not be optimal for the human ones. Alternatively, exothermic aggregation of the unfolded fragment or some other fast nonequilibrium postdenaturational processes that may accompany the unfolding may compensate the endothermic denaturation effect and shift the transition to a lower temperature. Nevertheless, whatever the explanation is, this result together with the CD data indicate the presence of compact structure in the COOH-terminal region of the human αC-domain. As in the case of the bovine connector, the human one also exhibited no heat absorption peak (Figure 6B, lower curve), suggesting the absence of compact structure in this region.

Structural Organization of the Connector Region. Although fluorescence and near-UV CD measurements revealed no compact structure in the αC-domain connector, one cannot exclude the possibility for the presence of some regular structures in this region. The most prominent feature of both bovine and human αC-connectors is the presence of tandem repeats of 13 amino acid residues enriched with Pro, Gly, Ser, and Thr (*26*). Taking into account that a number of proline-rich polypeptides and proteins with repetitive sequences adopt the extended left-handed helical conformation known as poly(L-proline) type II (PPII) (*27*), we hypothesized earlier that such conformation may be present also in the αC-connector (*28*). To test this hypothesis, we performed detailed analysis of the recombinant human and bovine connectors by CD and DSC, techniques that allow detection of some features characteristic for the PPII conformation.

The far-UV CD spectra of the isolated bovine and human connectors exhibited a negative maximum at 197−198 nm and a shoulder at 215−235 nm (insets in Figure 8 A,B). In both connectors, the amplitude of the negative maximum decreased while that of the shoulder increased at high temperature. When heated, both connectors exhibited a linear increase in ellipticity at 222 nm without any hint of a sigmoidal transition, but with a change of the slope at about 50−55 °C (Figure 8A,B). Linear extrapolation of the data before and after this region (dashed lines in Figure 8A,B) revealed inflection points at 50 and 55 °C for the bovine and human connectors, respectively. Such CD spectra and temperature-induced behavior of the CD signals at 222 nm are reminiscent of those reported for PPII (*29*−*31*). However, in both connectors, most repeats contain a Trp residue which may contribute to the same spectral region as PPII (*31*−*33*), thus complicating correct interpretation of the CD data. To address this, we synthesized a peptide (NPGSPRPGSTGT) corresponding to the sixth repeat of the human connector without its COOH-terminal Trp and performed

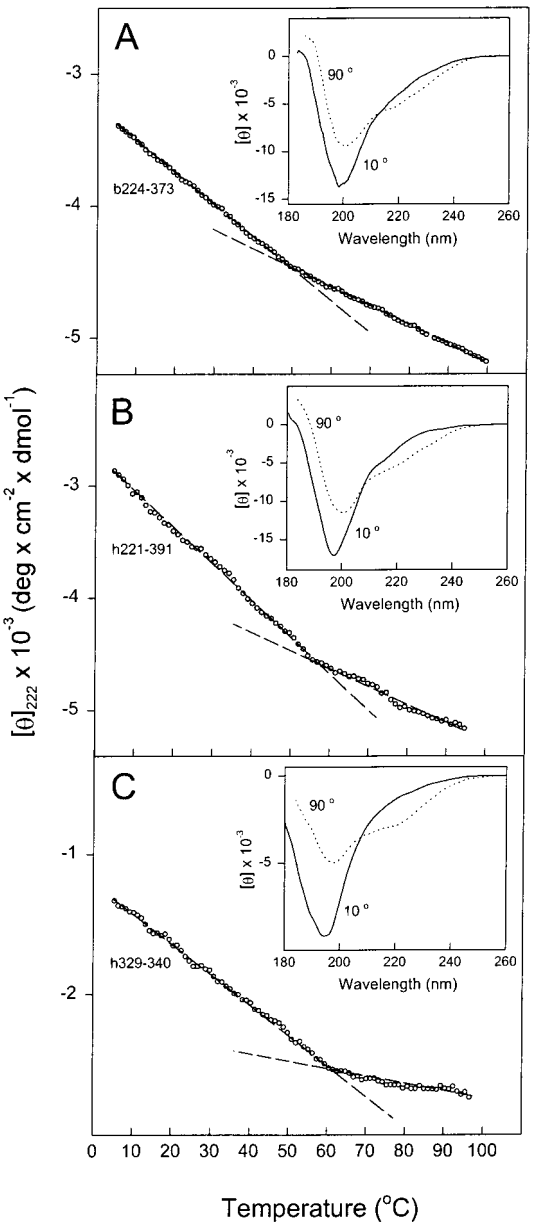

FIGURE 8: Heat-induced changes in ellipticity of the bovine and human connector fragments and the synthetic peptide detected by circular dichroism. Heat-induced changes in ellipticity at 222 nm are shown for the bovine b224−373 fragment (panel A), the human h221−391 fragment (panel B), and the synthetic peptide NPGSPRPGSTGT mimicking the sixth repeat (residues 329−340) of the human αC-connector (panel C). The insets represent CD spectra of the corresponding fragments and the peptide at 10 °C (solid lines) and 90 °C (dotted lines). All experiments were performed in 20 mM sodium phosphate buffer, pH 7.4. The dashed lines represent linear extrapolations of the CD values to determine the inflection points.

similar CD measurements (Figure 8C). Both the CD spectrum and the temperature-induced change in the ellipticity at 222 nm in this peptide were similar to those observed with the isolated connectors, suggesting that contribution of the Trp residues in this spectral region is negligible. Thus, the above CD data strongly suggest the presence of PPII in both connectors as well as in the synthetic repeat.

As mentioned above, when heated in the calorimeter, both connectors exhibited no heat absorption peak (lower curves in Figure 6A,B), indicating that they do not contain compact structure. At the same time, at low temperatures, the

measured heat capacity function (C_p) in both cases was lower than the theoretical C_p function for the unstructured connectors (dashed curves) calculated from the amino acid composition (see Experimental Procedures). This difference decreased with increasing temperature until the two C_p functions converged at 50−60 °C, in the same temperature range where the change in linear slope of the CD signals at 222 nm was observed (Figure 8). Again, such behavior of the C_p function is characteristic for polypeptides in the PPII conformation (*34*), reinforcing the above suggestion that the PPII conformation is present in both connectors.

DISCUSSION

The fibrin(ogen) αC-domains are involved in fibrin assembly (*35*−*37*), in controlling activation of factor XIII (*38*), and in cell adhesion via their Aα572−574 RGD sequence and via bound fibronectin (*39*−*41*). They also contain binding sites for tPA and plasminogen and cross-linking sites for α_2-antiplasmin and PAI-2 (*18*, *42*, *43*), which play a prominent role in regulation of fibrinolysis. It is not surprising that the molecular defects in the αC-domains of several congenitally abnormal fibrinogens result in disfibrinogenemia associated with defective thrombolysis (*44*, *45*). It was also reported that several mutations in the αC-domain result in hereditary renal amyloidosis, which is caused by deposition of the truncated αC-fragments in kidney (*46*, *47*). Despite their functional importance and substantial progress in establishment of the high-resolution structure of fibrinogen, the structural organization of the αC-domains is still unclear. On the one hand, it was hypothesized that the COOH-terminal half of the αC-domain forms a compact structure which is attached to the bulk of the molecule by the flexible NH_2-terminal connector region (*5*). On the other hand, a recent X-ray study of chicken fibrinogen crystals revealed no compact structure in this region of the molecule (*14*). The present study was performed to resolve these obvious contradictions and to clarify the structural organization of the αC-domain.

In contrast to the fibrinogen D and E fragments, which are highly resistant to proteolysis, the αC-domains are easily degraded into smaller fragments (*2*, *26*), creating difficulties in preparation and investigation of this important fibrinogen region. In our previous attempts to prepare the isolated αC-domain from plasmin digests of bovine fibrinogen, we faced two problems: first, only the αC-fragment with the truncated COOH-terminus was purified; and, second, the yield of the fragment was not sufficient for extensive structural studies (*15*). Others faced similar problems upon preparation of the αC-fragment from plasmin digests of human fibrinogen (*48*). To overcome these problems, we expressed human αC-domain and its variants in *E. coli* (*17*, *18*). The yield of the recombinant fragments was comparatively high, and their COOH-termini were preserved. However, a denaturation study did not provide convincing evidence for the presence of compact structure in those fragments (nonpublished results), suggesting either that the procedure used for their refolding required further modifications or that the αC-domain may indeed be unordered. That is why in this study we first focused on the refolding of the recombinant fragments. The expression of the bovine αC-domain and its variants facilitated solution of the refolding problem. The major advantage of the bovine αC-domain over the human one is the presence of a single Trp460 in its COOH-terminal region, which was hypothesized to be compact (*5*). This made possible the use of fluorescence spectroscopy, a less protein- and time-consuming method, for fast screening of a wide variety of refolding conditions and selecting those that yielded recombinant fragments with fluorescence spectra characteristic for a folded proteins.

While searching for better refolding conditions, we found that high concentrations of sodium chloride substantially improved the yield of the refolded full-length bovine αC-fragment (b224−568) and its COOH-terminal variants (b374−568 and b374−538). These fragments exhibited blue-shifted fluorescence spectra when compared to fully denatured proteins, suggesting the presence of a compact structure. More importantly, they exhibited fluorescence-detected sigmoidal transitions in response to heat and urea, which is the best evidence for a folded structure. The occurrence of the transition at higher temperature in higher salt concentration explained the enhancing effect of salt on refolding of the recombinant fragments. Further CD experiments in the near- and far-UV regions revealed similar heat-induced transitions connected with cooperative unfolding of the tertiary and secondary structures, respectively, reinforcing our conclusion about the presence of a compact structure in these fragments. More so, since the transitions in the full-length αC-fragment and in the COOH-terminal truncated variants had similar shape and enthalpy, we concluded that the compact structure is located in the COOH-terminal region of the αC-domain. In addition, thermodynamic analysis of the DSC-obtained endotherms revealed that this region is folded into a single cooperative unit (domain). CD and DSC measurements gave similar results with the full-length human αC-fragment (h221−610) and its COOH-terminal variant (h392−610) although the quality of the DSC data precluded their accurate thermodynamic analysis. This proves unambiguously our previous hypothesis (*5*) that the COOH-terminal region of the αC-domain is folded into a compact structure.

It is well established that the extreme 3 kDa COOH-terminal portion of the αC-domain is easily removed upon proteolysis of fibrinogen by plasmin (*2*, *36*, *49*). The cleavage in both human and bovine αC-domains occurs in a homologous position at residues 583−584 and 539−540, respectively (arrows in Figure 1A). To test the role of this portion in maintaining compact structure of the αC-domain, we compared the denaturation of the bovine b374−568 fragment with that of its truncated variant b374−538. The thermal stabilities of both fragments were similar, suggesting that the 3 kDa portion does not contribute noticeably to the stability of the compact COOH-terminal region of the αC-domain and thus may be unordered. This finding suggests that the truncated b374−538 fragment may contain less unordered structure and thus could be a better candidate for crystallization and further structural studies of the αC-domain by X-ray or by NMR.

The αC-domains in different species have different lengths, and their sequences vary significantly. This argument together with the high susceptibility of the αC-domains to proteolysis was used in support of unordered character of the αC-domain (*13*). At the same time, previous alignment of the αC-domain sequences from several mammalian species (*50*) and that presented in Figure 1A revealed that

the major variability in size is connected with the length of their NH_2-terminal connector region. In addition, although the alignment in Figure 1A gave only 46% identical residues in the COOH-terminal regions of bovine and human αC-domains including residues 392−610 and 374−568, respectively, they both are folded into a compact structure as revealed in this study. This argues that despite high sequence variability, the COOH-terminal regions of other species could also be compact. In this respect, the weak electron density in the region of the αC-domains reported for chicken fibrinogen (*13*) does not rule out the presence of a compact structure which retains some motional freedom in the crystal.

The structure of the connector region of the αC-domain is quite different from that of the compact COOH-terminal part. Both human and bovine connectors (residues 221−391 and 224−373, respectively) start with a 43−45 residue segment followed by a number of 13-residue internal tandem repeats, 10 in human and 8 in bovine (Figure 1A). The interspecies variability in the size of this region is mainly connected with variations in the number and length of such repeats. There are 13 such repeats in monkey and only 5 in mouse and some other rodents (*50*). The variability in nonmammalian species is even higher, from 18 repeats in lamprey to 0 in chicken (*51*, *52*). Although none of the methods used in this study revealed the presence of a compact structure in the isolated bovine and human connectors, they seem to be at least partially ordered. In fact, the data presented here strongly support our hypothesis (*28*) that this region contains an extended helical PPII conformation which most probably is formed by the tandem repeats. The presence of such conformation, which is thought to be stabilized by hydrogen bonds with water molecules (*27*), is consistent with an unusually high degree of hydration of the fibrinogen molecule reported long ago [(*53*) and references cited therein] but still unexplained. It is also consistent with the lack of success in crystallization of intact bovine fibrinogen containing tandem repeats and successful crystallization of chicken fibrinogen lacking such repeats (*13*, *54*) since the extended PPII structures are hard to crystallize (*27*). Finally, since proline-rich sequences and repeats utilize unique properties of PPII to carry out binding functions in many proteins (*27*), one can speculate that the connector region of the αC-domain may also interact via its tandem repeats with other fibrinogen domains or other proteins such as fibronectin (*55*).

In summary, the COOH-terminal region of each fibrinogen Aα chain, which is easily removed upon proteolysis (Aα221−610 in human and Aα224−568 in bovine), is traditionally called the αC-domain. However, this terminology does not reflect structural organization of this region since various data including those presented here indicate that each αC-domain consists of two structurally very distinct regions. The COOH-terminal half (Aα392−610 in human and Aα374−568 in bovine) forms an independently folded compact cooperative unit (domain) which was also revealed as a separate globular entity by electron microscopy (*7*, *8*). The NH_2-terminal half (Aα221−391 in human and Aα224−373 in bovine), containing a number of tandem repeats which are most probably in the extended helical PPII type conformation, forms a flexible region connecting the compact globular half to the bulk of the molecule. It seems to be reasonable to refer to the compact part as the αC-domain and the flexible part as the αC-connector.

ACKNOWLEDGMENT

We thank Dr. M. Murakawa for providing cDNA of the Aα chain of bovine fibrinogen and Dr. K. Ingham for helpful discussions and criticism.

REFERENCES

1. Doolittle, R. F. (1984) *Annu. Rev. Biochem. 53*, 195−229.
2. Henschen, A., and McDonagh, J. (1986) in *Blood Coagulation* (Zwaal, R. F. A., and Hemker, H. C., Eds.) pp 171−241, Elsievier Science Publishers, Amsterdam.
3. Privalov, P. L., and Medved, L. V. (1982) *J. Mol. Biol. 159*, 665−683.
4. Medved, L., Litvinovich, S., Ugarova, T., Matsuka, Y., and Ingham, K. (1997) *Biochemistry 36*, 4685−4693.
5. Medved, L. V., Gorkun, O. V., and Privalov, P. L. (1983) *FEBS Lett. 160*, 291−295.
6. Hall, C. E., and Slayter, H. S. (1959) *J. Biophys. Biochem. Cytol. 5*, 11−15.
7. Erickson, H. P., and Fowler, W. E. (1983) *Ann. N.Y. Acad. Sci. 408*, 146−163.
8. Weisel, J. W., Stauffacher, C. V., Bullitt, E., and Cohen, C. (1985) *Science 230*, 1388−1391.
9. Spraggon, G., Everse, S. J., and Doolittle, R. F. (1997) *Nature 389*, 455−462.
10. Everse, S. J., Spraggon, G., Veerapandian, L., Riley, M., and Doolittle, R. F. (1998) *Biochemistry 37*, 8637−8642.
11. Madrazo, J., Brown, J. H., Litvinovich, S., Dominguez, R., Yakovlev, S., Medved, L., and Cohen, C. (2001) *Proc. Natl. Acad. Sci. U.S.A. 98*, 11967−11972.
12. Brown, J. H., Volkmann, N., Jun, G., Henschen-Edman, A. H., and Cohen, C. (2000) *Proc. Natl. Acad. Sci. U.S.A. 97*, 85−90.
13. Yang, Z., Mochalkin, I., Veerapandian, L., Riley, M., and Doolittle, R. F. (2000) *Proc. Natl. Acad. Sci. U.S.A. 97*, 3907−3912.
14. Yang, Z., Kollman, J. M., Pandi, L., and Doolittle, R. F. (2001) *Biochemistry 40*, 12515−12523.
15. Veklich, Y. I., Gorkun, O. V., Medved, L. V., Nieuwenhuizen, W., and Weisel, J. W. (1993) *J. Biol. Chem. 268*, 13577−13585.
16. Procyk, R., Medved, L., Engelke, K. J., Kudryk, B., and Blomback, B. (1992) *Biochemistry 31*, 2273−2278.
17. Matsuka, Y. V., Medved, L. V., Migliorini, M. M., and Ingham, K. C. (1996) *Biochemistry 35*, 5810−5816.
18. Tsurupa, G., and Medved, L. (2001) *Biochemistry 40*, 801−808.
19. Studier, F. W., Rosenberg, A. H., Dunn, J. J., and Dubendorff, J. W. (1990) *Methods Enzymol. 185*, 60−89.
20. Edelhoch, H. (1967) *Biochemistry 6*, 1948−1954.
21. Gill, S. C., and von Hippel, P. H. (1989) *Anal. Biochem. 182*, 319−326.
22. Privalov, P. L., and Potekhin, S. A. (1986) *Methods Enzymol. 131*, 4−51.
23. Filimonov, V. V., Potekhin, S. A., Matveev, S. V., and Privalov, P. L. (1982) *Mol. Biol. (Moskow) 16*, 551−562.
24. Makhatadze, G. I., and Privalov, P. L. (1990) *J. Mol. Biol. 213*, 375−384.
25. Privalov, P. L., and Makhatadze, G. I. (1990) *J. Mol. Biol. 213*, 385−391.
26. Doolittle, R. F., Watt, K. W., Cottrell, B. A., Strong, D. D., and Riley, M. (1979) *Nature 280*, 464−468.
27. Williamson, M. P. (1994) *Biochem. J. 297 (Pt. 2)*, 249−260.
28. Weisel, J. W., and Medved, L. (2001) *Ann. N.Y. Acad. Sci. 936*, 312−327.
29. Makarov, A. A., Lobachov, V. M., Adzhubei, I. A., and Esipova, N. G. (1992) *FEBS Lett. 306*, 63−65.
30. Sreerama, N., and Woody, R. W. (1994) *Biochemistry 33*, 10022−10025.

31. Woody, R. W. (1992) *Adv. Biophys. Chem. 2*, 37−39.
32. Makarov, A. A., Esipova, N. G., Lobachov, V. M., Grishkovsky, B. A., and Pankov, Y. (1984) *Biopolymers 23*, 5−22.
33. Woody, R. W. (1994) *Eur. Biophys. J. 23*, 253−262.
34. Makarov, A. A., Adzhubei, I. A., Protasevich, I. I., Lobachov, V. M., and Esipova, N. G. (1993) *J. Protein Chem. 12*, 85−91.
35. Medved, L. V., Gorkun, O. V., Manyakov, V. F., and Belitser, V. A. (1985) *FEBS Lett. 181*, 109−112.
36. Gorkun, O. V., Veklich, Y. I., Medved, L. V., Henschen, A. H., and Weisel, J. W. (1994) *Biochemistry 33*, 6986−6997.
37. Cierniewski, C. S., and Budzynski, A. Z. (1992) *Biochemistry 31*, 4248−4253.
38. Credo, R. B., Curtis, C. G., and Lorand, L. (1981) *Biochemistry 20*, 3770−3778.
39. Cheresh, D. A., Berliner, S. A., Vicente, V., and Ruggeri, Z. M. (1989) *Cell 58*, 945−953.
40. Corbett, S. A., Lee, L., Wilson, C. L., and Schwarzbauer, J. E. (1997) *J. Biol. Chem. 272*, 24999−25005.
41. Corbett, S. A., and Schwarzbauer, J. E. (1998) *Trends Cardiovasc. Med. 8*, 357−362.
42. Sakata, Y., and Aoki, N. (1980) *J. Clin. Invest. 65*, 290−297.
43. Ritchie, H., Lawrie, L. C., Crombie, P. W., Mosesson, M. W., and Booth, N. A. (2000) *J. Biol. Chem. 275*, 24915−24920.
44. Lijnen, H. R., Soria, J., Soria, C., Collen, D., and Caen, J. P. (1984) *Thromb. Haemostasis 51*, 108−109.
45. Koopman, J., Haverkate, F., Grimbergen, J., Egbring, R., and Lord, S. T. (1992) *Blood 80*, 1972−1979.
46. Benson, M. D., Liepnieks, J., Uemichi, T., Wheeler, G., and Correa, R. (1993) *Nat. Genet. 3*, 252−255.
47. Uemichi, T., Liepnieks, J. J., and Benson, M. D. (1994) *J. Clin. Invest. 93*, 731−736.
48. Rudchenko, S., Trakht, I., and Sobel, J. H. (1996) *J. Biol. Chem. 271*, 2523−2530.
49. Cottrell, B. A., and Doolittle, R. F. (1976) *Biochim. Biophys. Acta 453*, 426−438.
50. Murakawa, M., Okamura, T., Kamura, T., Shibuya, T., Harada, M., and Niho, Y. (1993) *Thromb. Haemostasis 69*, 351−360.
51. Wang, Y. Z., Patterson, J., Gray, J. E., Yu, C., Cottrell, B. A., Shimizu, A., Graham, D., Riley, M., and Doolittle, R. F. (1989) *Biochemistry 28*, 9801−9806.
52. Weissbach, L., and Grieninger, G. (1990) *Proc. Natl. Acad. Sci. U.S.A. 87*, 5198−5202.
53. Doolittle, R. F. (1973) *Adv. Protein Chem. 27*, 1−109.
54. Cohen, C., Weisel, J. W., Phillips, G. N., Jr., Stauffacher, C. V., Fillers, J. P., and Daub, E. (1983) *Ann. N.Y. Acad. Sci. 408*, 194−213.
55. Makogonenko, E., Tsurupa, G., Ingham, K., and Medved, L. (2002) *Biochemistry* (in press).
56. Privalov, P. L. (1979) *Adv. Protein Chem. 33*, 167−241.

BI025584R